

Dusty Galaxies and AGNs in Quiescent Galaxy Candidates under NUV-r-J Selection



Yu-Hsuan Hwang 黃于瑄* (NTU, ASIAA), Wei-Hao Wang (ASIAA), Yu-Yen Chang (ASIAA), Chen-Fatt Lim (NTU, ASIAA)

*e-mail: r07222045@ntu.edu.tw

Motivation

- Observing the properties of quiescent galaxies (QGs) at different redshifts provides us insights about the rapid formation and quenching of massive galaxies in the early universe.
- The selection criteria based on color-color diagram are widely applied to selecting QGs, but the selected QGs may suffer from contamination by red dusty star-forming galaxies at high redshift. For instance, a $z = 3.7$ QG candidate (Glazebrook et al., 2017) was detected at $450 \mu\text{m}$ wavelength. This implied that the galaxy was a dusty star-forming galaxy (Simpson et al., 2017). Therefore, we include sub-millimeter data to measure the contamination among the selected QGs.
- Quenching mechanism of galaxies is an important issue under debate. We analyze the active galactic nucleus (AGNs) in our data by calculating the QG fraction among AGN samples, and the correlation between AGNs and QGs may provide a clue toward the quenching process in QGs.

Data

- We selected a sample of 173573 galaxies with robust photometric data from the multi-wavelength band-merged COSMOS2015 catalog (Laigle et al. 2016). Our samples cover an area of 2 deg^2 in the COSMOS field.
- 17271 galaxies, or 9.95% of the total sample size, were selected as QG candidates in the NUV-r-J diagram, with the criteria proposed by Ilbert et al. (2013): $M_{NUV} - Mr > 3(Mr - M_J) + 1$, and $M_{NUV} - M_r > 3.1$ (Fig. 1).
- We also cross-matched our samples with *Spitzer* MIPS 24- μm and VLA 3-GHz (Smolčić et al., 2017) for further analysis.

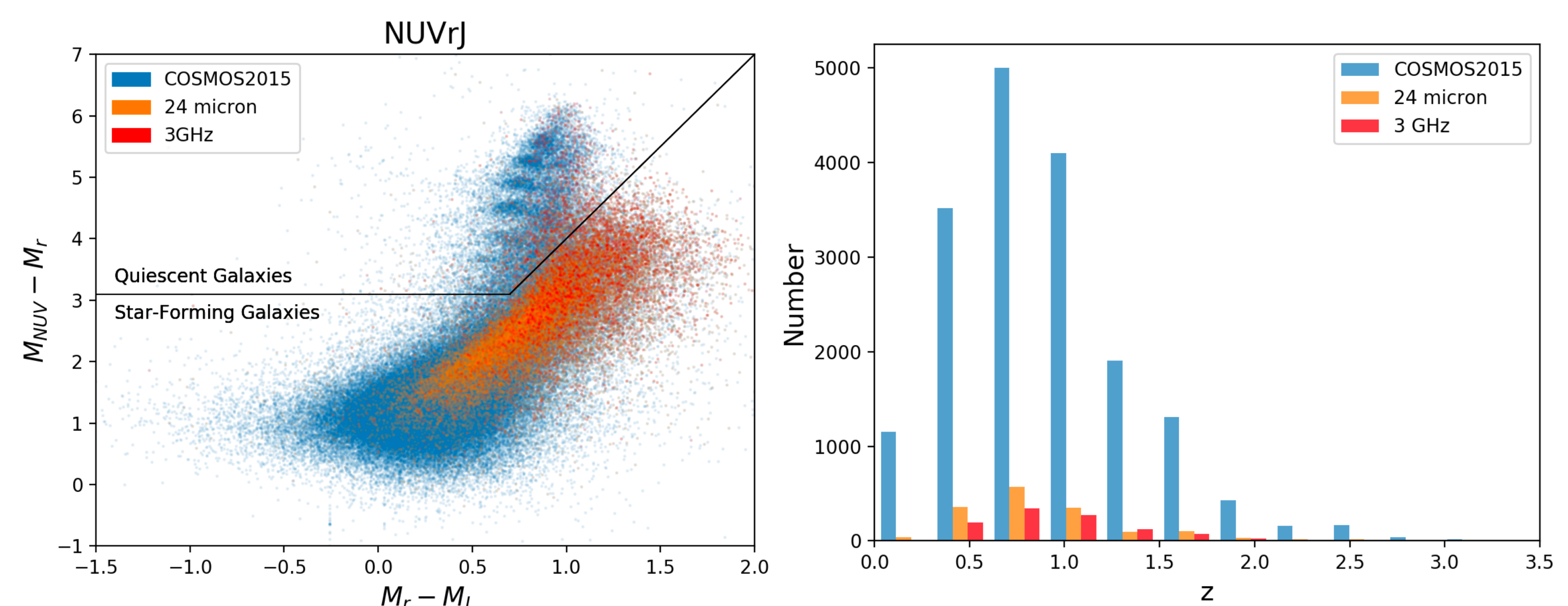


Fig 1: 17271 galaxies were selected as QG candidates in the NUV-r-J diagram (left). The selected QG candidates distribute out to redshifts around 3 (right).

Searching for Dusty galaxies

Finding Bright Sub-mm Sources with Cross-Matching

- We cross-matched our samples with JCMT SCUBA-2 450- μm (STUDIES; Wang et al. 2017) and 850- μm (S2COSMOS; Simpson et al., 2019) sources, with the help from high-resolution multi-wavelength data, including *Spitzer* MIPS 24- μm , VLA 3-GHz, and ALMA 870- μm source catalogs.
- Our result suggests that roughly 1% of our samples are bright submillimeter sources (Table 1).

Table 1: Results of cross-matching JCMT SCUBA-2 data.

wavelength	detection limit	area (deg ²)	sub-mm detected QGs	total QGs in the area	sub-mm detected QGs / total QGs
850 μm	$\sim 2 \text{ mJy}$	~ 2	13	17271	$0.2 \pm 0.03\%$
450 μm	$\sim 3.5 \text{ mJy}$	~ 0.13	8	1817	$2.0 \pm 0.7\%$

Finding Faint Sub-mm Sources with Stacking Analysis

- We excluded those directly detected submillimeter sources and perform stacking analysis. The remaining QG candidates still show emission at sub-mJy levels both in the SCUBA-2 450- μm map and 850- μm map (Table 2).
- We classified QG candidates either with 24- μm counterparts or with 3-GHz counterparts labeled with SFG flags in the VLA catalog as “dusty SFGs.” We find that the stacked fluxes are especially high for the dusty SFGs, which account for 8.2% and 9.4% of the total QGs, respectively, for the 450- μm and 850- μm map. We conclude that the contamination by faint submillimeter sources is at a roughly 10% level.
- Our stacked fluxes in the 450- μm image are lower than the results using Herschel data at 500- μm wavelength (Man et al., 2016) by a factor of 10. This suggest that the stacked fluxes in the Herschel image may be biased by source blending and clustering due to poor resolution.

Table 2: Results of stacking JCMT SCUBA-2 data.

Groups	850 μm image				450 μm image			
	number	mean flux (mJy)	SNR	% among all QGs	number	mean flux (mJy)	SNR	% among all QGs
All QGs	17248	0.08 ± 0.01	8.3	-	1809	0.11 ± 0.06	2.0	-
Dusty SFG	1421	0.35 ± 0.03	10.2	8.2%	170	0.71 ± 0.18	3.9	9.4%
Non-dusty SFG	15827	0.06 ± 0.01	5.6	91.8%	1639	0.06 ± 0.02	1.0	90.6%

Properties of AGN Samples

QG Fraction in AGN Samples

- We cross-matched our samples with radio AGNs, mid-infrared AGNs, and X-ray AGNs (Table 3). The stellar mass of the samples were limited to above 10^{11} solar mass to avoid incompleteness of the observation and to make a fair comparison. We calculated the QG fraction in different classes of AGN samples and in different redshift bins (Fig. 2).
- The QG fraction of radio AGNs are higher than that of the entire COSMOS2015 samples up to around redshift 1.5. Our data implies that AGN activities, particularly radio jets, play an important role in the quenching process in QGs.

Table 3: Different classes of AGNs.

AGN	data	definition
Radio AGN	VLA catalog (Smolčić et al. 2017)	radio excess over 3σ in $\log(L_{1.4\text{GHz}}/SFR_{\text{IR}})$
Mid-infrared AGN	COSMOS2015 catalog (Chang et al. 2017)	rest-frame mid-IR color-color diagram
X-ray AGN	<i>Chandra</i> data (Civano et al. 2016, Marchesi et al. 2016)	$L_x(2-10\text{keV}) > 10^{42} \text{ ergs/s}$

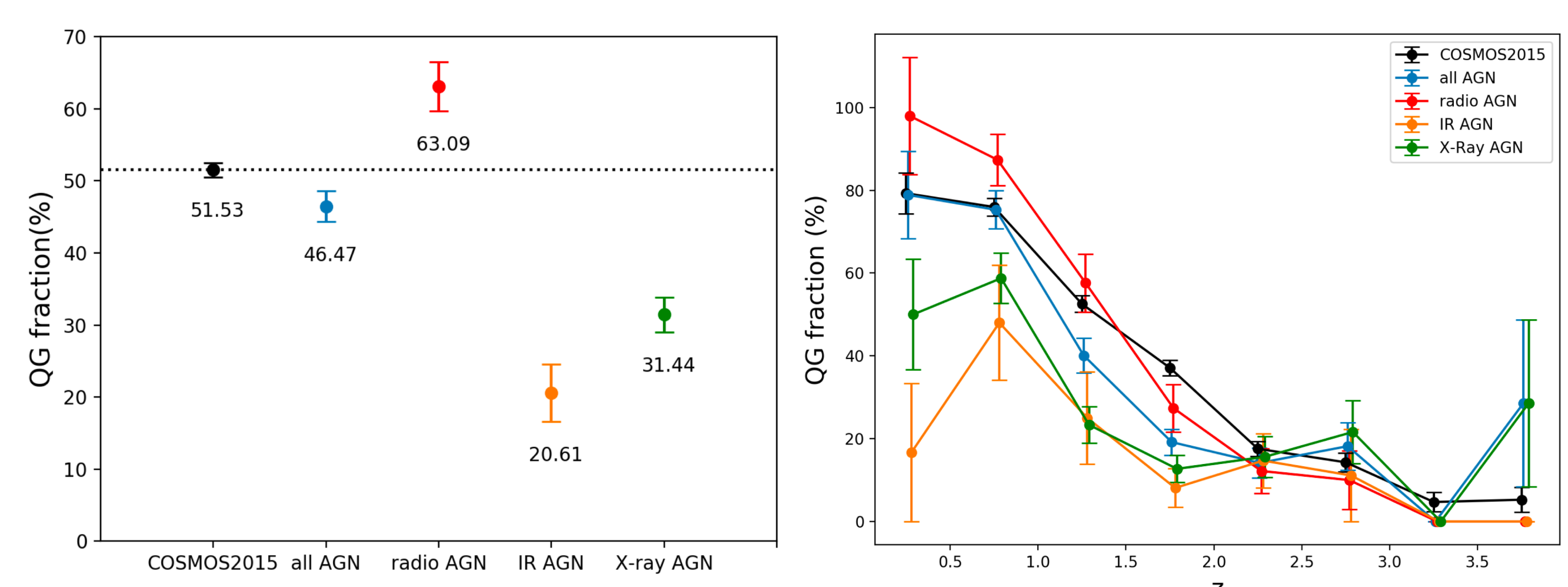


Fig 2: The QG fraction among different classes of AGN samples (left) and in different redshift bins (right). The samples were limited to $M_* > 10^{11} M_{\odot}$. The black dotted line in the left panel shows the QG fraction among the entire COSMOS2015 samples.

Conclusion

We analyze a sample of 17271 color-selected quiescent galaxies (QGs) in the NUV-r-J diagram. We find that roughly 1% and 10% of our QG candidates are contaminated by bright and faint submillimeter detected dusty galaxies respectively. We find a strong correlation between QGs and radio AGNs, which may suggest a connection between quenching mechanism and radio-mode AGN feedback.